NUMERICAL INVESTIGATION ON THE EFFECT OF INCIDENT SHOCK WAVE ON MIXING AND COMBUSTION OF TRANSVERSE HYDROGEN INJECTION IN SUPERSONIC AIRSTREAM

Y. Shoraka* and S. Tabejamaat*
yshoraka@aut.ac.ir
* Aerospace Engineering Department, Amirkabir University of Technology, Tehran, IRAN

Abstract
The present study describes the numerical investigation of the effect of incidence shock wave interaction on mixing and combustion of transverse hydrogen injection. Therefore, the second – order implicit upwind TVD scheme in conjunction with local characteristic approach is used for the simulation of unsteady multidimensional chemical reacting flow in a generalized coordinate. The species equations and the convective fluid dynamic equations are solved in a coupled fully implicit form with the LU scheme. The numerical scheme employs Baldwin-Lomax algebraic turbulence model. Hydrogen and air combustion is simulated by means of a full chemical mechanism. Obtained results indicated that without incident shock wave auto ignition of the hydrogen jet occurs in high temperature airstream. Nevertheless the flame will subsequently quenched downstream of the injector. When the incident shock wave introduced upstream of the injector flameholding could not be achieved. On the other hand, the flame stabilization is confirmed when the incident shock wave is introduced downstream of the injector.

Introduction

As is illustrated in Fig 1, Scramjet engines have high specific impulse at high Mach number. Unlike rockets, Scramjets don't need to store oxidizer that generally comprises 65% payload of rockets' takeoff weight. Moreover, unlike ramjets, air dissociation doesn't occur in their combustor for supersonic flights above Mach 5. Hence, being very efficient air-breathing propulsion systems, they are indispensable for the future of aerospace industry [1,2].

A crucial element in the development of Scramjets is its supersonic combustor, whereas, due to a short duration of time for mixing and burning, achieving stable combustion inside their combustion chamber is a cumbersome task. In this regard, most of the research activity on the development of scramjets is focused on the study of supersonic combustion in their combustors. To achieve a stable combustion, residence time of fuel inside the scramjet combustor must be increased in order to obtain enough time for the mixing of the fuel and air. Combustor's geometry, type of the fuel and injection model play an important role in achieving a sustainable combustion [3].

Since hydrogen produces more specific impulse (As depicted in Fig. 1) and has smaller characteristic combustion time in comparison with hydrocarbon fuels; it is the most efficient fuel for using in scramjet engines.

In regard to combustor's geometry various methods have been developed for increasing the residence time of fuel inside scramjet's combustor. One solution is to implement a geometrical obstruction inside the combustor. Examples of these geometrical obstructions are backward facing step [4] and cavity [5].

As mentioned above, apart from the geometrical obstructions and characteristic combustion time the other important factor in flameholding is the type of fuel injection. Fuel injection can be categorized into two approaches; transverse injection from an injector located on the well or in stream injection from struts. Transverse injection results in rapid mixing, therefore this type of injection can enhance flame stabilization [6]. Hence transverse injection has been studied extensively [7-12].

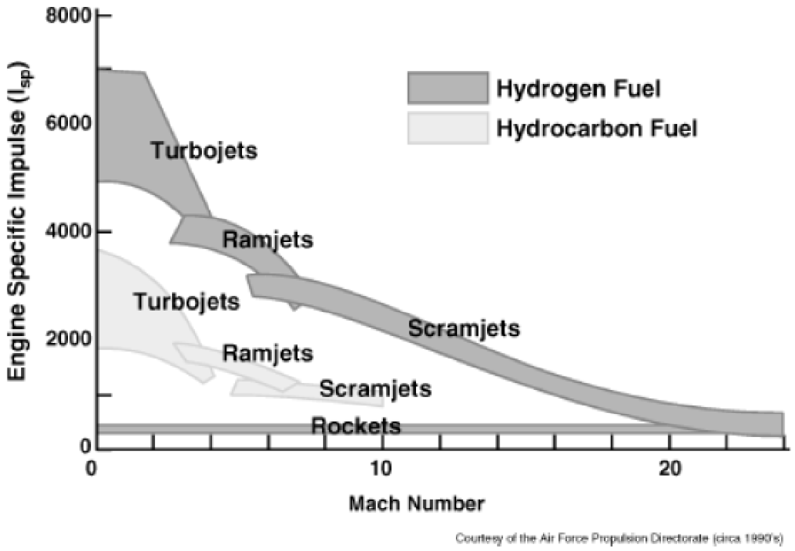

Figure 1. Specific Impulse Versus Mach Number for Various Engine Types [3]

Since the air stream condition entering the scramjet combustion substantially changes, due to the wide operational range of hypersonic vehicles; many incident shock waves may occur inside the scramjet's combustor. Therefore, the interaction between fuel injection and the incident shock wave is an important factor in the control of supersonic combustion. Moreover, the strength and the location of the incident shock wave may change drastically, which could make supersonic combustion uncontrollable [2].

Ratner et al. have studied the interaction between the shock wave and axisymmetric hydrogen jet. Their studies revealed that adding shockwaves causes a significant decrease in the combustion efficiency of the flames, which they studied [13]. Rubins et al. studied shock-induced combustion. They demonstrated that the air-fuel mixture can be ignited by passing it through a normal or oblique shock wave [14]. Kim et al. investigated the effect of shock waves on the supersonic hydrogen–air jet flame stabilized in a Mach 2.5 circular cross-section combustor. Their study revealed that shock waves create a radially inward/outward air flow to the flame and elongate a flame-holding recirculation zone, and thus fuel–air mixing is enhanced significantly, resulting in improved combustion efficiency [15]. Yang et al. numerically investigated unsteady shock induced vortical flows. The flows consist of one or more regions of light gas, surrounded by heavy gas, being overtaken by a normal shock wave. The interaction of the density gradient at each light/heavy interface with the pressure gradient from the shock wave generates vorticity. This causes the light gas regions to roll up into one or more counter-rotating vortex pairs, which stir and mix the light and heavy gases [16]. Although, transverse injection has been established to be an efficient scheme for supplying fuel in scramjet's combustor, and has been vastly studied by researchers [7-12], little work has been done to understand the fundamental mechanism of the interaction between the incident shock wave and transverse injection. Recently Mai et al. have shown that introducing the incident shock wave downstream the injection slot enhances the mixing and combustion of the traversal injection of hydrogen jet [2]. The aim of the current research is to investigate the effect incident shock wave impingement upstream and downstream of the injector on the flow field, mixing and combustion of a transversal hydrogen jet in comparison with the case that no incident shock is present.

Governing Equations

The conservative form of the non-dimensional Favre-averaged governing equations for compressible fluid flow comprise the Navier-Stokes, energy and species transport equations in general coordinates can be represented by relations (1)-(6) [17].

$$\frac{\partial \hat{U}}{\partial t}+\frac{\partial \hat{F}_j}{\partial \xi_j}=\frac{1}{\mathrm{Re}_0}\frac{\partial \hat{F}v_j}{\partial \xi_j} \tag{1}$$

$$\hat{F}_j=\begin{bmatrix} \tilde{\rho}_k \bar{U}_j ; k=1..9 \\ \tilde{\rho}\tilde{u}_1 \bar{U}_j+\frac{\partial \xi_j}{\partial \tilde{x}_1}\tilde{P} \\ \tilde{\rho}\tilde{u}_2 \bar{U}_j+\frac{\partial \xi_j}{\partial \tilde{x}_2}\tilde{P} \\ \tilde{\rho}\tilde{u}_3 \bar{U}_j+\frac{\partial \xi_j}{\partial \tilde{x}_3}\tilde{P} \\ (\tilde{E}+\tilde{P})\bar{U}_j \end{bmatrix} \tag{2}$$

$$\hat{F}v_j=\begin{bmatrix} \tilde{\rho}(\tilde{D}_k+\tilde{D}_t)\left(\frac{\partial \xi_j}{\partial \tilde{x}_i}\frac{\partial \tilde{Y}_k}{\partial \tilde{x}_i}\right); k=1..9 \\ \frac{\partial \xi_j}{\partial \tilde{x}_i}\tilde{\tau}_{1i} \\ \frac{\partial \xi_j}{\partial \tilde{x}_i}\tilde{\tau}_{2i} \\ \frac{\partial \xi_j}{\partial \tilde{x}_i}\tilde{\tau}_{3i} \\ \frac{\partial \xi_j}{\partial \tilde{x}_i}(\tilde{u}_l\tilde{\tau}_{il}+\tilde{q}_i) \end{bmatrix} \tag{3}$$

$$\bar{U}_j=\frac{\partial \xi_j}{\partial \tilde{x}_i}\tilde{u}_i \tag{4}$$

$$\tilde{\tau}_{ij}=(\tilde{\mu}+\tilde{\mu}_t)\left(\frac{\partial \tilde{u}_i}{\partial \tilde{x}_j}+\frac{\partial \tilde{u}_j}{\partial \tilde{x}_i}-\frac{2}{3}\delta_{ij}\frac{\partial \tilde{u}_k}{\partial \tilde{x}_k}\right) \tag{5}$$

$$\tilde{q}_j=\frac{\tilde{\mu}_t}{\mathrm{Pr}_t}\left(\frac{\partial \tilde{h}}{\partial x_j}\right)+\tilde{\lambda}\frac{\partial \tilde{T}}{\partial \tilde{x}_j}+<\tilde{\rho}>\sum_{k=1}^{NS}\tilde{h}_k\tilde{D}_k\frac{\tilde{Y}_k}{\partial \tilde{x}_j} \tag{6}$$

In order to close the system of equations, the gas mixture pressure is defined by the following equation

$$\tilde{P}=\tilde{\rho}\tilde{R}\tilde{T} \tag{7}$$

Where the gas constant for a mixture of gases can be derived by the following equation

$$\tilde{R} = \frac{R}{C_{p0}} = \frac{R_u}{C_{p0}} \sum_{k=1}^{NS} \frac{Y_k}{W_k} \tag{8}$$

The enthalpy of each species is calculated incorporating equation (9), where h_k^o is the enthalpy of formation of each species

$$h_k = h_k^o + \int_{T_{ref}}^{T} Cp_k dT \tag{9}$$

In equation (9), Cp_k represents the specific heat capacity for species k and is estimated by the equation (10) where it is defined by a fourth order polynomial equation of temperature from JANAF tables [18].

$$Cp_k = \sum_{i=0}^{4} a_{ik} T^i \tag{10}$$

In this study, viscosity of species k is determined from equation (11) [19].

$$\mu_k = 2.6693*10^{-6} \frac{\sqrt{W_k T}}{\sigma_k^2 \Omega_k^{(2.2)}} \tag{11}$$

Thus, the viscosity of gas mixture can be calculated from Wilke's formula [20] that is represented by

$$\mu = \sum_{i=1}^{NS} \frac{\mu_i}{1 + \sum_{k=1, k \neq i}^{NS} \frac{X_k}{X_i} \varphi_{ik}} \tag{12}$$

Where

$$\phi_{ik} = \frac{1}{2\sqrt{2}} \left(1 + \frac{W_i}{W_k}\right)^{-0.5} \left[1 + \left(\frac{\mu_i}{\mu_k}\right)^{0.5} \left(\frac{W_i}{W_k}\right)^{0.25}\right] \tag{13}$$

The following equation is used to calculate the thermal conductivity of each species [21]

$$\lambda_k = 8.323*10^{-3} \frac{\sqrt{T/W_k}}{\sigma_k^2 \Omega_k^{(2.2)}} + 1.32 \frac{\mu_k}{W_k} (Cp_k - 2.5 R_k) \tag{14}$$

The thermal conductivity of mixture is calculated using equation [22]

$$\lambda = \sum_{i=1}^{NS} \frac{\lambda_i}{1 + \sum_{k=1, k \neq i}^{NS} 1.065 (X_k \varphi_{ik})} \tag{15}$$

The diffusion coefficient for each species is derived from equation (14) by assuming Lewis number equal to 1 [17].

Numerical Scheme

In order to solve the governing equations for turbulent supersonic flows, second order Harten-Yee symmetric TVD scheme with min-mod limiter [23] is used to calculate inviscid terms, while the viscous terms are calculated by the second order central difference scheme. The difference equation is then integrated in time by incorporating LU scheme [24]. In all calculation CFL=0.5 was used for the first thousand iterations and then higher CFL numbers are issued to achieve steady state solution. In order to accelerate the solution, and reduce computational costs, local time stepping is implemented.

Turbulence Modelling

The turbulent component for viscosity is calculated, using the algebraic eddy viscosity model that is developed by the Baldwin and Lomax [25]. Whereas, those for thermal conductivity and diffusion coefficient are obtained from turbulent component of viscosity by using fixed turbulent Prandtl and Schmidt numbers equal to 0.9 and 0.5 respectively in order to improve the numerical accuracy [26]. Although, it has been reported that Baldwin-Lomax model might be unreliable in the simulation of flow fields with separation, since the objective of the current study was qualitative analysis, this model is used because of its simplicity and computational efficiency. However, it is still needed to incorporate more reliable turbulence models, which will be considered in further investigations.

Chemical Reaction Model

A full chemical mechanism for hydrogen and air combustion consists of 9 – species, 37 – step reaction proposed by Stahl and Warnatz [27] is used to calculate species production rate by laminar chemistry approach. Although this approach ignores turbulence-chemistry interaction, recent investigations revealed that the effect of turbulence-chemistry interactions is relatively minor except in the vicinity of flame ignition for supersonic combustion [28].

Code Verification

In order to validate the implemented numerical method, a problem of transverse injection into supersonic airstream is considered following the experimental configuration of Spaid and Zukoski [7].

The computational domain for this case is a rectangular consists of a flat plate with a slot located 228.6 mm downstream of the wall's leading edge at the bottom, supersonic inlet at the left with free stream Mach number of 3.5, total pressure of 2.41 bar and total temperature of 314 K, supersonic outlet at right and finally a far-field boundary on the top. The width of the slot is 0.2667 mm where a sonic nitrogen jet with total pressure of 3.8 bar and total temperature of 292 K is injected transversely into the free stream.

At supersonic inlet, all the conservative variables are set regarding the given data for the free stream. At supersonic outlet, the conservative variables are extrapolated at the second-order from the upstream values. The flat plate is assumed to be an adiabatic wall where velocity is zero (no-slip condition); pressure is extrapolated from the values above the plate.

Three grid systems of 161 × 55, 181 × 65, 201 × 85 are generated. The grid density is clustered towards wall and injection port for all grids and relaxed towards top and outlet.

In Fig. 2, the surface pressure distribution obtained from all three grid systems are plotted and compared with experimental data. As depicted in Fig. 2, apart from the location of boundary layer separation upstream of the injector, grid convergence is achieved. Since the results obtained by 161*55 grid system are reasonable in comparison with experimental data, this grid system is used for further computations.

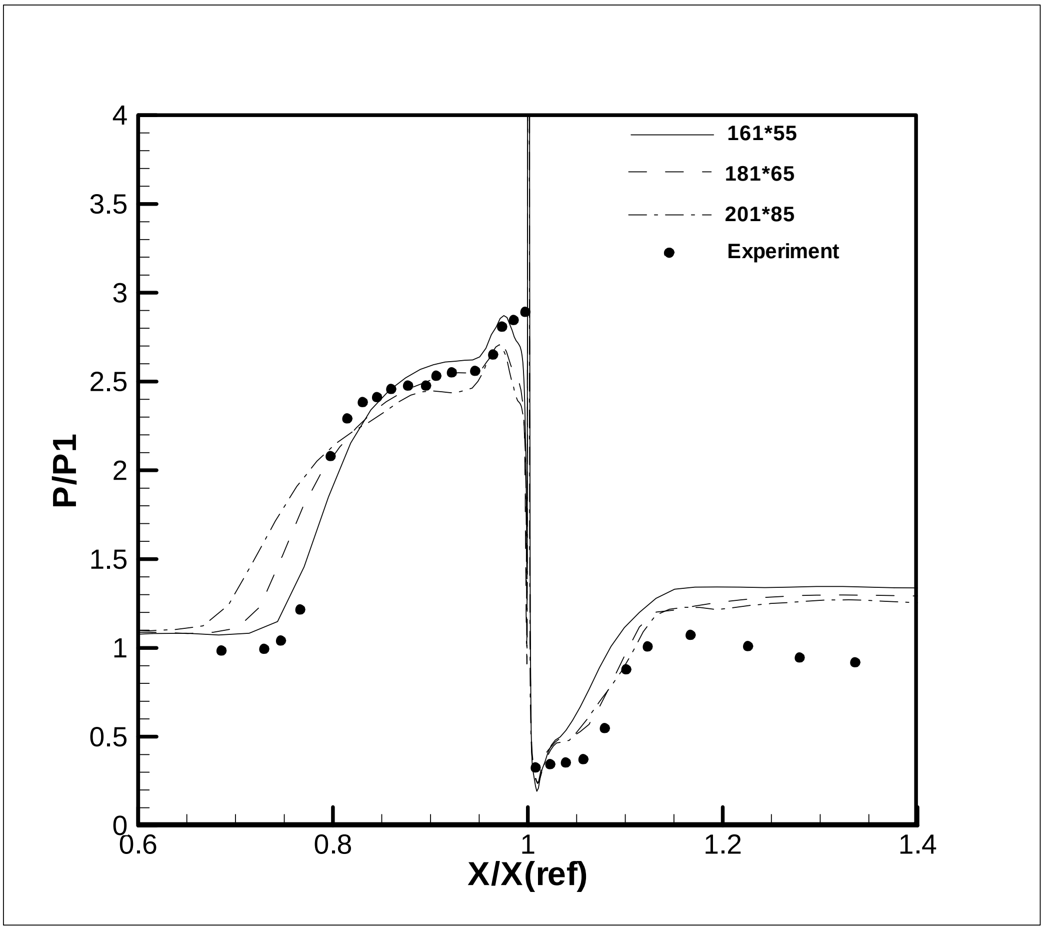

Figure 2. Wall Pressure distribution for the case of transverse injection into airstream

Results and Discussion

Based on the above validation, the numerical method described in the previous sections is applied to the computation of shock wave/transversal injection interaction. As schematically shown in Fig. 3, the computational domain for this case, following the experimental configuration of Nakamura [29], is a rectangular consists of a flat plate, whose length is 180.5 mm, with a slot located 100 mm downstream of the wall's leading edge at the bottom, supersonic inlet with free stream Mach number of 2.5, static pressure of 29263.7 Pa and static temperature of 320 K and 550 K for cold and hot airstreams respectively, at the left and supersonic outlet at the right.

Following the experimental data, the width of the slot is 0.5 mm where a sonic hydrogen jet with static pressure of 581088.2 Pa and static temperature of 300 K is injected transversely into the free stream.

At supersonic inlet, all the conservative variables are set regarding the given data for the free stream. At supersonic outlet, the conservative variables are extrapolated at the second-order from the upstream values. The flat plate is assumed to be an adiabatic wall where velocity is zero (no-slip condition); pressure is extrapolated from the values above the plate.

Experimentally, the oblique shockwave is generated using a wedge which deflects the incoming supersonic flow; numerically, it is sufficient to impose the incoming supersonic state on the left side of the top plane while another supersonic state is imposed on the right side of the top plane. This state is computed so as to satisfy the Rankine–Hugoniot relations across a shock with the given upstream state and shockwave angle [30].

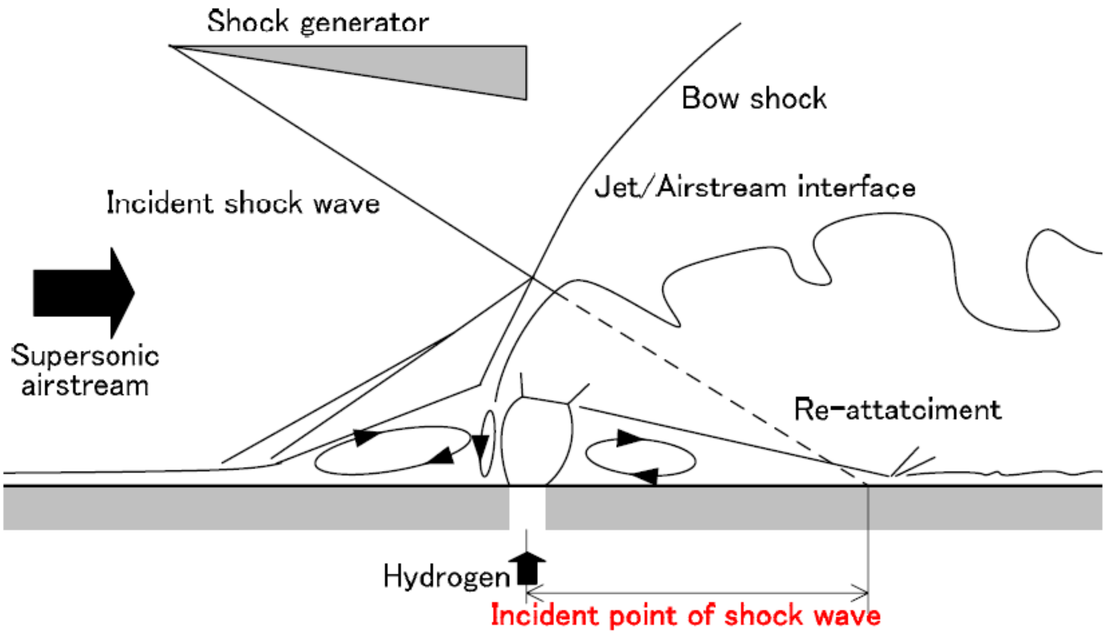

Figure 3. Computational geometry

Figs. 4 and 5 illustrate the computed flow field and Mach number contours distribution without incident shock wave. As is shown in Figs 4 and 5, the transverse jet acts like an obstruction on the main flow. This blockage results in a strong jet-induced bow shock. As the result if the adverse pressure gradient imposed on the turbulent boundary layer by the bow shock, boundary layer separates upstream of the injector which leads to the formation two counter rotating vortices as is shown in Fig 4. As depicted in Fig. 6, the formation of these counter rotating vortices causes the injected fuel to be sucked into the recirculation region upstream of the injector. As shown in Fig. 7, In the case of hot mainstream flow, auto ignition will occur in this region, nevertheless the flame quenches downstream.

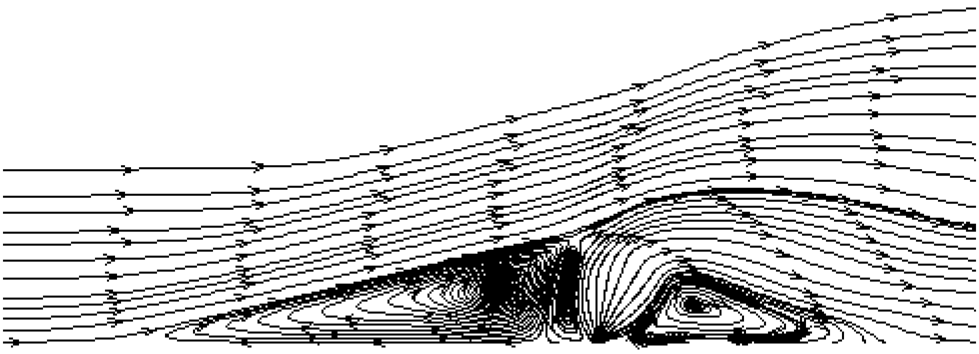

Figure 4. Flow field without incident shock wave

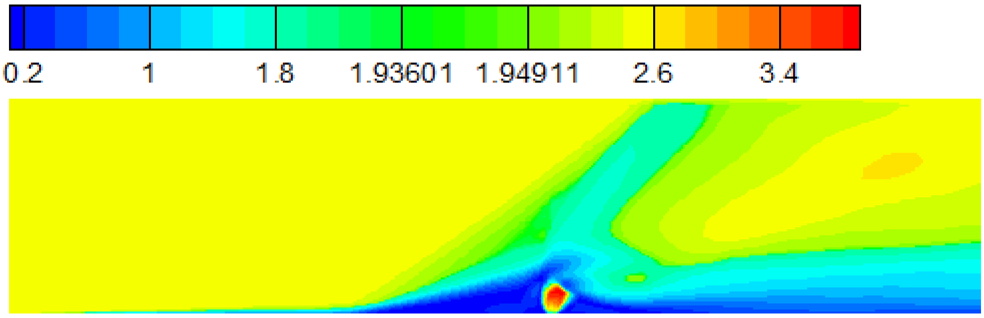

Figure 5. Mach number contours distribution without incident shock wave.

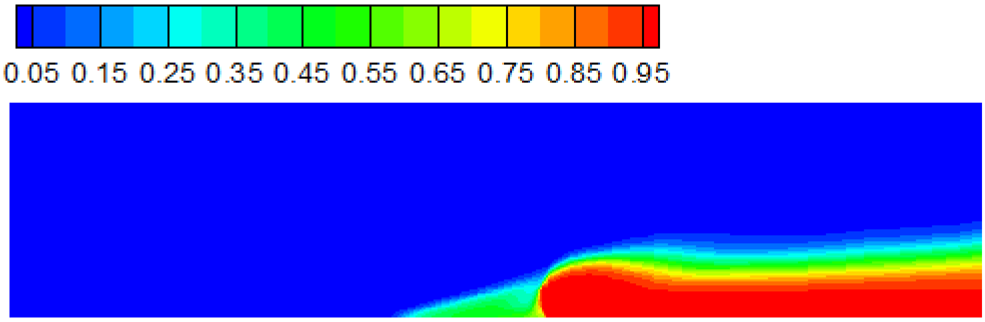

Figure 6. Hydrogen mass fraction contours distribution without incident shock wave.

The obtained numerical results are consistent with those observed experimentally by Ben-Yaker et al. [31].

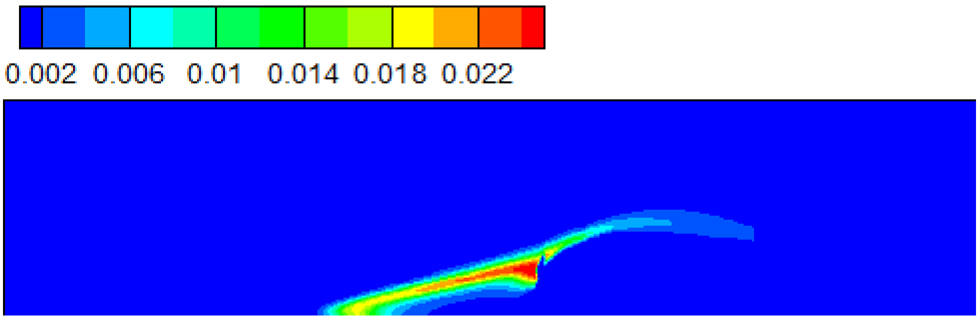

Figure 7. OH mass fraction contours distribution without incident shock wave.

Figs. 8 and 9 illustrate the computed flow field and Mach number contours distribution with incident shock wave introduced upstream of the injector. As is shown in Figs 8 and 9, the incident shock wave distorts the flow field drastically and enlarges the recirculation region upstream of the injector.

Figure 8. Flow field with incident shock wave introduced upstream of the injector

However, As shown in Fig. 10, the injected fuel will not be sucked into the recirculation region upstream of the injector in this case. Therefore, no flame was observed in the case of hot mainstream flow

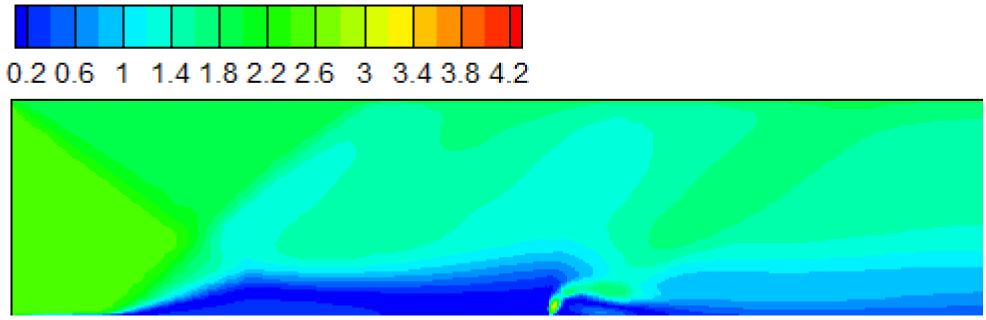

Figure 9. Mach number contours distribution with incident shock wave introduced upstream of the injector

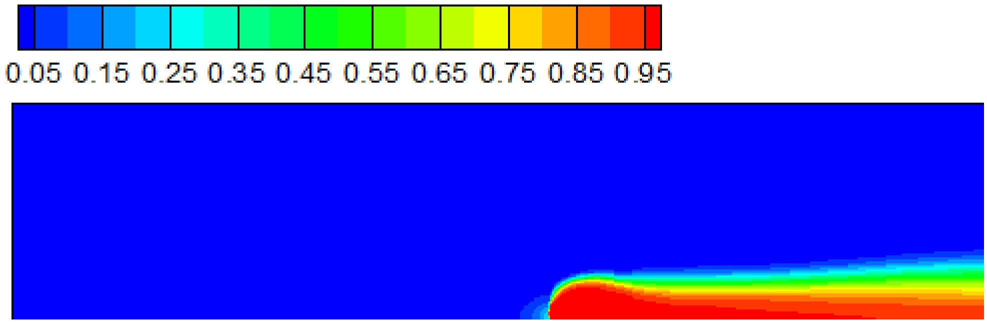

Figure 10. Hydrogen mass fraction contours distribution with incident shock wave introduced upstream of the injector

Figs. 11 and 12 illustrate the computed flow field and Mach number contours distribution with incident shock wave introduced downstream of the injector. As is shown in Figs 11 and 12, the incident shock wave distorts the flow field drastically as in the case where incident shock wave was introduced upstream of the injector.

Although the recirculation region upstream of the injector is smaller in this case in comparison with case without incident shockwave, As shown in Fig. 13, the injected fuel will also be sucked into the recirculation region upstream of the injector in this case. However, as illustrated by OH mass fraction distribution in Fig. 13, a sustainable combustion is observed in this case which is consistent with experimental and numerical results obtained by previous researches [2].

Figure 11. Flow field with incident shock wave introduced downstream of the injector

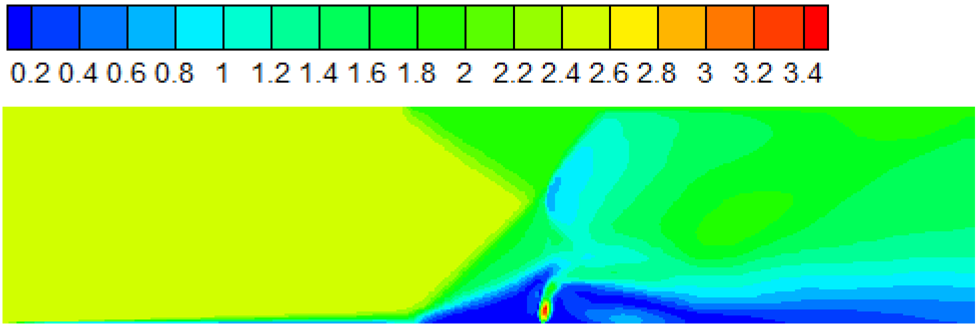

Figure 12. Mach number contours distribution with incident shock wave introduced downstream of the injector

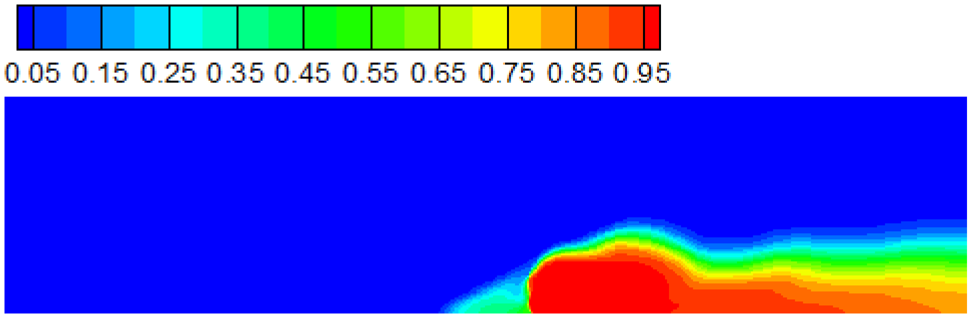

Figure 13. Hydrogen mass fraction contours distribution with incident shock wave introduced downstream of the injector

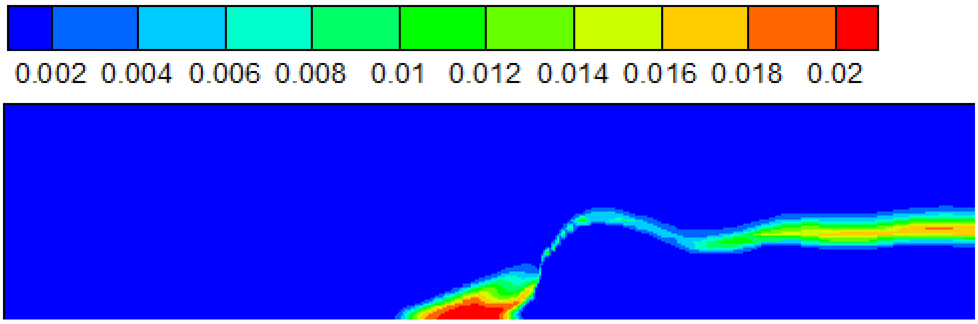

Figure 14. OH mass fraction contours distribution with incident shock wave introduced downstream of the injector

Conclusion

The present study revealed that without incident shock wave the injected hydrogen is sucked into the recirculation zone just upstream of the injector that would create a suitable zone for auto ignition of the hydrogen jet in high temperature airstream. Nevertheless the flame will subsequently quenched downstream of the injector which is consistent with experimental results [31]. When the incident shock wave introduced upstream of the injector, the flow field distorts drastically, and, fuel is no more present in the recirculation region just upstream of the injector. Therefore flame stabilization could not be achieved in this case. When the incident shock wave introduced downstream of the injector, the flame stabilization is confirmed which is consistent with previous experimental and numerical observations [2].

References

[1] Heiser, W. H., Prat, D. T., *Hypersonic Air breathing Propulsion*, AIAA, 1994, pp. 14-22

[2] Mai, T., Sakimitsu, Y., Nakamura, H., Ogami, Y., Kudo, T., Kobayahi., H., “Effect of incident shock wave interacting with transversal jet flow on the mixing and combustion”, *Proc. Comb. Inst.* 33:2335-2342 (2011).

[3] Builder, C., H., Prat, D. T., “On Thermodynamic Spectrum of Airbreathing Propulsion” *Proc AIAA 1st Annual Meeting,* Washington, D. C., AIAA Paper 64-243 (1964).

[4] Akhgari, M., Tabejamaat, S., Seraj Mehdizadeh, “Numerical Study of The Effect of injection Modeling on Mixing and Flame Stability in Supersonic Combustion”, *Comb. Sci. and Tech.* 179: 281-291 (2007).

[5] Ben-Yakar, A., Hanson R. K., “Cavity Flame Holders for Ignition and Flame Stabilization in Scramjet: An Overview”, *Journal of Propulsion and Power* 17:869-877, (2001).

[6] Drummond, J. P., Diskin, G. S., Culter A. D., “Fuel-Air Mixing and Combustion in Scramjets” *Proc AIAA 1st Annual Meeting,* Washington, D. C., AIAA Paper 64-243.

[7] Spaid, F. W., Zukoski E. E., “A Study of the Interaction of Gasous Jets from Transverse Slots with Supersonic External Flows”, *AIAA J.* 6:205-211, (1968).

[8] Gruber, M. R., Nejad A. S., Chen T. H., Dutton J. C., “Mixing and Penetration Studies of Sonic Jets”, *Journal of Propulsion and Power* 11:315-323, (1995).

[9] Gruber, M. R., Nejad A. S., Chen T. H., Dutton J. C., “Transverse Injection from Circular and Elliptic Nozzles into a Supersonic Cross flow”, *Journal of Propulsion and Power* 16:449-457, (2000).

[10] Viti, V., Neel, R., Schetz, J. A., “Detailed flow physics of the supersonic jet interaction flow field”, *Physics of Fluids* 21, (2009).

[11] Karagozian, A. R., “Transverse jets and their control”, *Progress in Energy and Combustion Science* 36:531-553, (2010).

[12] Erdem, E., Kontis, K., “Numerical and experimental investigation of transverse injection flows”, *Shock Waves* 20:103-118, (2010).

[13] Ratner, A., Driscoll, J. F., Huh, H., Bryant, R. A. “Combustion Efficiencies of Supersonic Flames”, *Journal of Propulsion and Power* 17:301-307, (2001).

[14] Rubins, R. M., Bauer, R. C., “Review of Shock-Induced Supersonic Combustion Research and Hypersonic Applications”, *Journal of Propulsion and Power* 10:593-601, (1994).

[15] Kim, J. H., Youngbin, Y., Jeung I. S., Huh, H., Choi, J. Y., “Numerical Study of Mixing Enhancement by Shock Waves in Model Scramjet Engine”, *AIAA J.* 41:1074-1080, (2003).

[16] Yanh, J., Kubota, T., Zukoski E. E., “Applications of Shock-Induced Mixing to Supersonic Combustion”, *AIAA J.* 31:854-862, (1993).

[17] Shoraka, Y., *Numerical Study of High Speed Reacting Flows by Developing a Three-Dimensional Code*, PhD Dissertation, Amirkabir University of Technology, Tehran, 2008.

[18] Chase, J. et al., *JANAF Thermochemical Tables,* 3rd Edition, pp. 14.

[19] White, F. M., *Viscous Fluid Flow,* McGraw-Hill Inc., New York, 1974, pp. 28.

[20] Svehla, R. A., “Estimated Viscosities and Thermal Conductivities of Gases at High Temperature” *NASA Technical Report R – 132.*

[21] Wilke, C. R., “A Viscosity Equation for Gas Mixtures”, *Journal of Chemical Physics* 18:517, (1950).

[22] Mason, E. A., Saxena, S. C., “Approximate Formula for the Thermal Conductivity of Gas Mixture”, *Physics of Fluids* 1:361, (1985).
[23] Yee, H. C., Harten, A., “Implicit TVD Schemes for Hyperbolic Conservation Laws in Curvilinear Coordinates”, *AIAA J.* 25:266-274, (1987).
[24] Shuen, J. S., Yoon, S., “Numerical Study of Chemically Reactiong Flows Using a Lower-Upper Symmetric Successivve Overrelaxation Scheme”, *AIAA J.* 27:1752-1756, (1988).
[25] Baldwin, B., Lomax, H., “Thin Layer Approximation and Algebraic Model for Separated Turbulent Flows”, AIAA Paper 78-257 (1978).
[26] Riggins, D. W., McClinton, C. R., “A Computational Investigation of Flow Losses in a Supersonic Combustor”, AIAA Paper 90-0293 (1990).
[27] Stahl, G., Warnatz, J., “Numerical Investigation of Time – Dependent Properties and Extinction of Strained Methane and Propane Air Flamelets”, *Combustion and Flame* 85:285, (1991).
[28] Baurle, R. A., “Modeling of High Speed Reacting Flows: Established Practices and Future Challenges”, *Proc 42nd AIAA Aerospace Sciences Meeting and Exhibit*, Reno, AIAA Paper 2004-267 (2004).
[29] Nakamura, H., *Study of Combustion of a Hydrogen Jet in Supersonic Flow Using PTV*, PhD Dissertation, Tohoku University, 2007.
[30] Boin, J. P., Robinet, J. C., Corre, C., Deniau, H., “3D steady and unsteady bifurcations in a shock-wave/laminar boundary layer interaction : a numerical study”, *Theor. Comput. Fluid. Dyn.* 20:163-180, (2006).
[31] Ben-Yakar, A., Hanson, R. K., “Experimental Investigation of Flame-Holding Capability of Hydrogen Transverse Jet in Supersonic Cross-Flow”, *Proc. Comb. Inst.* 27:2173-2180 (1988).